https://doi.org/10.5194/acp-2019-1128
Preprint. Discussion started: 16 March 2020

Atmospheric Chemistry and Physics Discussions

Numerical analysis of the impact of agricultural emissions on $PM_{2.5}$ in China using a high-resolution ammonia emissions inventory

Xiao Han[1,2], Lingyun Zhu[5], Mingxu Liu[4], Yu Song[4] Meigen Zhang[1,2,3],

[1]*State Key Laboratory of Atmospheric Boundary Layer Physics and Atmospheric Chemistry, Institute of Atmospheric Physics, Chinese Academy of Sciences, Beijing 100029, China*

[2]*College of Earth and Planetary Sciences, University of Chinese Academy of Sciences, Beijing 100049, China*

[3]*Center for Excellence in Urban Atmospheric Environment, Institute of Urban Environment, Chinese Academy of Sciences, Xiamen 361021, China*

[4]*State Key Joint Laboratory of Environmental Simulation and Pollution Control, Department of Environmental Science, Peking University, Beijing 100871, China.*

[5]*Shanxi Province Institute of Meteorological Sciences, Taiyuan 030002, China*

Corresponding author:

Lingyun Zhu

Shanxi Province Institute of Meteorological Sciences

Xinjian Road 65#, Taiyuan, Shanxi province, China

Post code: 030002

Tel: 86-0351-4077738

Fax: 86-0351-4077738

E-mail: zhlyun@126.com

Meigen Zhang

LAPC, Institute of Atmospheric Physics, Chinese Academy of Sciences

HuaYanBeiLi 40#, Chaoyang District

Beijing, China

Post code: 100029

Tel: 86-010-62379620

Fax: 86-010-62041393

E-mail: mgzhang@mail.iap.ac.cn

https://doi.org/10.5194/acp-2019-1128
Preprint. Discussion started: 16 March 2020

Atmospheric Chemistry and Physics Discussions

Abstract

China is one of the largest agricultural countries in the world. The NH_3 emissions from agricultural activities in China significantly affect regional air quality and horizontal visibility. To reliably estimate the influence of NH_3 on agriculture, a high-resolution agricultural NH_3 emissions inventory, compiled with a 1 km × 1 km horizontal resolution, was applied to calculate the NH_3 mass burden in China. The key emission factors of this inventory were enhanced by considering the results of many native experiments, and the activity data of spatial and temporal information were updated using statistical data from 2015. Fertilizer and husbandry, as well as farmland ecosystems, livestock waste, crop residue burning, fuel wood combustion, and other NH_3 emission sources were included in the inventory. Furthermore, a source apportionment tool, ISAM (Integrated Source Apportionment Method), coupled with the air quality modeling system RAMS-CMAQ (Regional Atmospheric Modeling System and Community Multiscale Air Quality), was applied to capture the contribution of NH_3 emitted from total agriculture (Tagr) in China. The aerosol mass concentration in 2015 was simulated, and the results showed that a high mass concentration of NH_3, which exceeded 10 μg m^{-3}, appeared mainly in the North China Plain (NCP), Central China (CNC), the Yangtz River Delta (YRD), and the Sichan Basin (SCB), and the annual average contribution of Tagr NH_3 to $PM_{2.5}$ mass burden in China was 14-18%. Specific to the $PM_{2.5}$ components, Tagr NH_3 provided a major contribution to ammonium formation (87.6%) but a tiny contribution to sulfate (2.2%). In addition, several brute-force sensitivity tests were conducted to estimate the impact of Tagr NH_3 emissions reduction on the $PM_{2.5}$ mass burden. Compared with the results of ISAM, it was found that even though the Tagr NH_3 only contributed 10.1% of nitrate under current emissions scenarios, the reduction of nitrate could reach 98.8% upon removal of the Tagr NH_3 emissions. The main reason for this deviation could be that the NH_3 contribution to nitrate is small under "rich NH_3" conditions and large in "poor NH_3" environments. Thus, the influence of NH_3 on nitrate formation could be enhanced with the decrease of ambient NH_3 mass concentration.

https://doi.org/10.5194/acp-2019-1128
Preprint. Discussion started: 16 March 2020

Atmospheric Chemistry and Physics Discussions

1. Introduction

Ammonia (NH_3) is an important pollution species which principal neutralizing agent for the acid aerosols, SO_4^{2-} and NO_3^- formed from the SO_2 and NO_x (Chang, 1989; McMurry et al.; 1983). In addition, NH_3 also influences the rate of particle nucleation (Ball et al.; 1999; Kulmala et al.; 2002) and enhances secondary organic aerosols (SOA) yields (Babar et al.; 2017). The widespread haze events have frequently occurred in most regions of eastern China in recent years, and several studies have reported that the secondary inorganic salts, including sulfate, nitrate, and ammonium, were the majorities of the total aerosols in the urban and rural regions (Tao et al.; 2014; Wang et al.; 2016; Zhang et al.; 2012; Lai et al.; 2016; Zhang et al.; 2018). Therefore, besides the heavy emissions of SO_2 and NO_2, NH_3 emissions from the agriculture activities are also non-negligible.

China is one of the largest agricultural countries in the world. Even though the annual emissions budget of NH_3 decreased from 2006 to 2012, the emissions were still high and reached 9.7-12 Tg (Kang et al., 2016; Xu et al., 2016; Zhou et al., 2015), leading to high ambient NH_3 concentrations. These massive NH_3 levels significantly affect regional air quality and horizontal visibility. Firstly, the major $PM_{2.5}$ components, $(NH_4)_2SO_4$, $(NH_4)_3H(SO_4)_2$, NH_4HSO_4, and NH_4NO_3 were partially or fully produced from the neutralization of H_2SO_4 and HNO_3 by the reaction with NH_3 (Tanner et al.; 1981; Brost et al.; 1988; Quan et al.; 2014; Zhao et al.; 2013; Zhang et al.; 2014). Studies also showed that NH_3 improves the H_2SO_4 nucleation by 1-10 times (Benson et al.; 2011), and provides sufficient new particle to alter the number and size distributions. Thus, the NH_3 and its secondary product NH_4^+ play an important role in the formation of air pollution and haze days. Research has shown that approximately 80% of total anthropogenic NH_3 emissions derived from agricultural sources and livestock manure provided a greater contribution than synthetic fertilizer (Kang et al., 2016; Zhou et al., 2016). The Chinese government has undertaken several control strategies to reduce particulate pollution and its precursors, such as catalytic reduction systems in the power sector (Xia et al., 2016), measures to change coal to gas for residential life and heating (Ren et al., 2014), etc. Related observations have shown that the mass burdens of SO_2 and NO_x have decreased distinctly in recent years (De Foy et al., 2016; Wang et al., 2015; Zheng et al., 2018). However, no specific measures for agricultural NH_3 emissions control have been implemented to date, and the total agricultural NH_3 emissions budget did not change substantially from 2010 to 2017 (Zheng et al., 2018).

In addition, accurate information on agricultural NH_3 emissions is also important for estimating the NH_3 mass burden and its environmental effect. There have been several studies focusing on NH_3 emissions

https://doi.org/10.5194/acp-2019-1128
Preprint. Discussion started: 16 March 2020


Atmospheric Chemistry and Physics Discussions

from agricultural activities in China or East Asia. REAS (Regional Emission inventory in Asia) version 2 established an anthropogenic emissions inventory that included the source of agricultural NH_3 (fertilizer application and livestock) (Kurokawa et al.; 2013). This inventory, targeting years from 2000 to 2008, has a 0.25° × 0.25° spatial resolution with monthly variation. MASAGE_NH_3 (Magnitude and Seasonality of Agricultural Emissions model for NH_3) was used to develop a bottom-up NH_3 emissions inventory by using the adjoint of the GEOS-Chem chemical transport model (Paulot et al.; 2014). The inverse of the network data for NH_4^+ wet deposition fluxes from 2005-2008 was used to optimize the NH_3 emissions in China in this inventory. Fu et al. (2015) used the CMAQ (Community Multiscale Air Quality) model coupled to an agro-ecosystem, which could obtain hourly emissions features by online model calculation, to estimate NH_3 emissions in 2011 with high spatial and temporal resolution. These NH_3 emissions inventories provided very useful datasets for understanding the distribution features of the NH_3 mass burden in China. However, with population migration, economic growth, and the increased consumption of agricultural products, the spatial distribution and strength of agricultural NH_3 emissions has significantly changed in China during the last decade (Xu et al., 2017), so that reliable emissions information based on recent years is also necessary for estimating the NH_3 mass burden.

Previous studies have investigated the influence of NH_3 emissions on aerosol loading in several typical areas of China. Wu et al. (2008) conducted sensitivity studies to assess the impact of livestock-produced NH_3 emissions on $PM_{2.5}$ mass concentration in North China by using the MM5/CMAQ modeling system. The results showed that the livestock-produced NH_3 provided >20% contributions to nitrate and ammonium, but provided only a small contribution to sulfate. Wang et al. (2011) used the response surface modeling technique to estimate the contribution of NH_3 emissions in East China and found that total NH_3 emissions contributed 8-11% to $PM_{2.5}$ concentration, and the nonlinear effects were significant while the transition between NH_3 rich and poor conditions. Fu et al. (2017) and Zhao et al. (2017) also investigated the impact of NH_3 emissions on $PM_{2.5}$ in East China and the Hai River Basin. However, the related studies were few and focused mainly on local regions; furthermore, most of them generally used the brute-force sensitivity method to estimate the NH_3 impact based on the chemistry model, which reflected the change in particulate concentration with emissions reduction (Koo et al., 2009).

PKU-NH_3, a comprehensive high-resolution NH_3 emissions inventory based on the year 2015, was applied in this study to capture the agricultural NH_3 mass concentration in China, and the contribution to $PM_{2.5}$ particles was estimated with an RAMS-CMAQ air quality modeling system, coupled with the online

https://doi.org/10.5194/acp-2019-1128
Preprint. Discussion started: 16 March 2020

Atmospheric Chemistry and Physics Discussions

source tagged module ISAM. Compared with previous studies, this high-resolution agricultural NH_3 emissions inventory was more accurate and reflected the latest spatial and temporal distribution features (Liu et al.; 2019). The major trace gases and aerosol species in 2015 were simulated by the modeling system and evaluated by several observational data. The contribution to the pollutant concentrations was tagged and quantified by RAMS-CMAQ-ISAM under the current scenario (Wang et al., 2009). Then, several brute-force sensitivity tests were conducted to estimate the effect of reducing agricultural NH_3 emissions on the $PM_{2.5}$ mass burden. The results from the source apportionment simulation and brute-force sensitivity tests in January, April, July, and October are presented here, and the detailed features over seven major populated areas of China (as shown in Figure 1) are discussed.

2. Methodology

The emissions inventory can be described as follows: First, the NH_3 emissions data in China were provided by the PKU-NH_3 emissions inventory (Kang et al., 2016; Zhang et al., 2018). This inventory was developed on the basis of previous studies (Huang et al., 2012) and improved the horizontal resolution and accuracy. It was compiled at a 1 km × 1 km horizontal resolution, with monthly statistical data from 2015. Some of the most uncertain parameters, the emission factors applied in this inventory, were enhanced by considering as many native experiment results as possible, with ambient temperature, soil acidity, and changes in other factors. In addition, this inventory not only included fertilizer and husbandry emissions from agricultural activities but also collected the emissions data of farmland ecosystems, livestock waste, biomass burning (forest and grassland fires, crop residue burning, and fuel wood combustion), and other sources (excrement waste from rural populations, the chemical industry, waste disposal, NH_3 escape from thermal power plants, and traffic sources). Second, the anthropogenic emissions of primary aerosols and their precursors were obtained from the MIX Asian emission inventory (base year 2012), prepared by the Model Inter-Comparison Study for Asia (MICS-ASIA III) (Lu et al., 2011; Lei et al., 2011). The anthropogenic emissions sources of SO_2, NO_x, volatile organic compounds (VOCs), black carbon (BC), organic carbon (OC), primary $PM_{2.5}$, and PM_{10} were obtained from the monthly MIX inventory, with a 0.25° × 0.25° spatial resolution. The REAS (Regional Emission Inventory in Asia; Version 2; Kurokawa et al., 2013) and GFED (Global Fire Emissions Database; Version 3; van der Werf et al., 2010) were used to provide the VOCs, and nitrogen oxides from flight exhaust, lightning, paint, wildfires, savanna burning, and slash-and-burn agriculture.

https://doi.org/10.5194/acp-2019-1128
Preprint. Discussion started: 16 March 2020

Atmospheric Chemistry and Physics Discussions

The RAMS-CMAQ modeling system was applied to simulate the transformation and transport of pollutants in the atmosphere. The CMAQ regional air quality model (version 5.0.2) released by the US Environmental Protection Agency (Eder et al., 2009; Mathur et al., 2008) was a major component of the RAMS-CMAQ modeling system. In this model, the CB05 (version CB05tucl) chemical mechanism (Whitten, 2010) and the sixth-generation CMAQ aerosol model (AERO6) were used to treat the gas-phase chemical mechanism and the formation and dynamic processes of aerosols. The ISORROPIA model (version 2.1) (Fountoukis and Nenes, 2007) was used to describe the thermodynamic equilibrium of gas-particle transformation. The highly versatile RAMS numerical model, which can well capture the boundary layer and the underlying surface, was applied to provide the meteorological fields for CMAQ (Cotton et al., 2003). The European Centre for Medium-Range Weather Forecasts reanalysis datasets (1° × 1° spatial resolution) were used to supply the background fields and sea surface temperatures. The model domain (Figure 1) was 6654 km × 5440 km, with 64 km^2 fixed-grid cells, and a rotated polar stereographic map projection covering the entire mainland of China and its surrounding regions was used. The model had 15 vertical layers, and half of them were located in the lowest 2 km to provide a more precise simulation of the atmospheric boundary layer. Several previous studies have demonstrated that the modeling system performs well when simulating the spatial and temporal distribution of China's major aerosol components (Han et al., 2013, 2014, 2016).

The ISAM is a flexible and efficient online source apportionment implementation, which was used to track multiple pollutants emitted from different geographic regions and source types. Compared with its previous version TSSA (Tagged Species Source Apportionment), the processes of tracking tagged tracer transport and precursor reactions were optimized for balancing the computational requirements and reliable representation of the physical and chemical evolution. To reduce the nonlinear effect during phase transformation and relative chemical interactions, a standalone subroutine "wrapper" approach was applied to the ISAM model to apportion the secondary PM species and their precursor gases during the thermodynamic equilibrium simulation; a hybrid approach, which employed the LU decomposition triangular matrices (Yang et al., 1997), was also developed for describing the gas-phase chemical interactions. In this study, ISAM was coupled with RAMS-CMAQ and was set to trace the transport and chemical reactions of NH_3 from fertilizer and husbandry emissions sectors to quantitatively estimate the contribution of agricultural NH_3 emissions to the $PM_{2.5}$ mass concentration in China.

https://doi.org/10.5194/acp-2019-1128
Preprint. Discussion started: 16 March 2020

Atmospheric Chemistry and Physics Discussions

3. Model evaluation

To evaluate the model performances, several observation data were compared with the simulation results. The meteorological factors are important to capture the formation processes and transport of secondary aerosols. Thus, in this paper, the observed meteorological data from surface stations of the Chinese National Meteorological Center are collected to evaluate the performance of the model. The detail information is described in Appendix A. Furthermore, the observed SO_2, NO_2, and $PM_{2.5}$ released from the Ministry of Environmental Protection of China were applied to evaluate the modeled mass concentration of these pollutants. The observation data at 416 stations, located in 101 model grids (distributed in Beijing, Tianjin, Hebei, Shandong, Shanxi, Henan, Jiangsu, and Anhui), were collected, and the values in same grid were averaged. The scatter plots of comparison are shown in Figure 2, and the statistical parameters between the observations and simulations are listed in Table 1. It can be seen that most of the scatter points broadly gather around the 1:1 solid line. The correlation coefficients in this table are all higher than 0.5, which indicates that the model can capture the regional variation in the measurements. The standard deviations between the observations and simulations were similar in most cases, except for SO_2 in January. The largest deviation of the modeled mean, which was higher than that of the observation, was also between the observed and modeled SO_2 in January. However, the correlation coefficients reached 0.71 in January, and the performance of the model in other months was relatively good, as shown in Table 1. It can be deduced that the obvious deviation may be a systemic underestimation due to the lack of emission intensity in this month.

The horizontal distributions of modeled monthly NH_3 mass concentration in January, April, July, and October in 2015 are shown in Figure 3. Pan et al. (2018) provided the distributions of satellite NH_3 total column distribution and the surface NH_3 concentrations at several observation sites (as shown in Figure 1 in the aforementioned study). As shown from their results, the highest mass burden was concentrated mainly in the North China Plain (NCP), Central China (CNC), the Yangtz River Delta (YRD), and the Sichan Basin (SCB). The simulation results in this study broadly reflected these distribution features. The NH_3 concentrations in these regions reached 10-25 μg m^3 in Pan et al. (2018), which also coincided well with the simulation results. However, some obvious deviations appeared in the eastern part of Gansu province. The modeled NH_3 in these regions was slightly higher than that of the observations in Pan et al. (2018). Zhang et al. (2018) also showed the NH_3 mass concentration in four seasons over China from simulation (horizontal distribution) and ground-based measurements (point values) in Figure 9 of their

https://doi.org/10.5194/acp-2019-1128
Preprint. Discussion started: 16 March 2020


Atmospheric Chemistry and Physics Discussions

study. Aside from the regions mentioned in Pan et al. (2018), the high mass burden of NH_3 also appeared in the NEC, as shown by both simulation and observation results in Zhang et al. (2018). Generally, this distribution feature should be reasonable because the Three River Plain located in NEC is an important agriculture base in China, and the NH_3 emissions in this region can be strong during spring and summer. The simulation results in this study also supported the seasonal variation of the NH_3 mass burden shown in Zhang et al. (2018), which was higher in summer and lower in winter, and the magnitudes of the two were close. Thus, it can be seen that the NH_3 concentration modeled by RAMS-CMAQ was reliable and can be applied to the analysis in this study.

4. Results and discussions

The horizontal distributions of modeled monthly $PM_{2.5}$ mass concentrations in January, April, July, and October 2015 are shown in Figure 4. Over the eastern part of China, the heavy $PM_{2.5}$ pollution occurred in January, and the relatively better air quality appeared in July. The large $PM_{2.5}$ mass burden, exceeding 200 μg m^3 in January, was mainly concentrated in the NCP, the Yangtze River Valley of CNC, and the SCB, which broadly coincided with the regions covered by a high mass burden of NH_3, as shown in Figure 3. In addition, the $PM_{2.5}$ mass burden (50-150 μg m^{-3}) was obviously lower in July than in the other months. Since NH_3 concerns mainly with secondary inorganic aerosols: sulfate, nitrate, and ammonium (SNA) formation, the analysis hereafter will mainly focus on the SNA. Figure 5 presents the modeled monthly SNA mass concentrations in January, April, July, and October 2015. The mass loading of SNA generally contributed 40-60% of the total $PM_{2.5}$ in the eastern part of China, which was comparable with previous studies (Cao et al., 2017; Chen et al., 2016; Lai et al., 2016; Wang et al., 2016). The distribution pattern and seasonal variation of SNA also followed the features of $PM_{2.5}$, and the high mass concentration of SNA exceeded 100 μg m^{-3} in January.

Then, the contributions of NH_3 from multiple agricultural emissions (including fertilizer, husbandry, farmland ecosystems, livestock waste, crop residue burning, and excrement waste from rural populations) to aerosols were calculated using RAMS-CMAQ-ISAM; the monthly average contribution percentage of total agriculture activities (Tagr) in January, April, July, and October are shown in Figure 6. Generally, Tagr NH_3 provided a 30-50% contribution to the SNA over most of eastern China in January and October, and a 20-40% contribution in April and July. The relatively lower value appeared mainly in April. The regional and annual average percent contributions of Tagr to sulfate, nitrate, ammonium, SNA, and $PM_{2.5}$ are shown

https://doi.org/10.5194/acp-2019-1128
Preprint. Discussion started: 16 March 2020

Atmospheric Chemistry and Physics Discussions

in Table 2. As shown in this table, Tagr NH_3 provided the major contribution to ammonium, which reached approximately 90%, and a relatively small contribution to nitrate mass burden, which was 5-10%. However, the contribution to sulfate was tiny, and the main reason is that there are various methods of sulfate formation from SO_2 other than neutralization by NH_3, such as oxidation by H_2O_2, O_3, or peroxyaceticn acid. Tagr NH_3 provided a 28-37% contribution to the SNA mass concentration, and the spatial features of the Tagr NH_3 contribution to the $PM_{2.5}$ mass concentration were similar to the features of SNA. Generally, it provided an approximately 14-18% contribution to the total $PM_{2.5}$ mass concentration in these places, and the largest annual average contribution appeared in CNC (17.5%).

In addition, the brute-force method (zero-out sensitivity test), which can capture the effect of emissions changes on aerosol mass burden, was applied to investigate the impact of the removal of Tagr NH_3 emissions. Unlike online source apportionment, the brute-force method mainly reflects the disparity of the chemical balance caused by the emissions change, which could significantly alter secondary pollutant formation. Several sensitivity tests were conducted, and the results are shown in Figure 7 and Table 3. Figure 7 presents the mass burden variation of SNA associated with Tagr NH_3 removal. From Figure 7, it can be seen that the reduction patterns of the aerosol broadly followed those of their mass burden. The significant reduction of SNA mainly appeared in the high concentration regions, and generally exceeded 25 μg m^{-3}. Table 3 shows the percentage of the variation of sulfate, nitrate, ammonium, SNA, and $PM_{2.5}$. Compared with Table 2, it can be seen that the variation percent of SNA and $PM_{2.5}$, which reached 40-51% and 23-35%, respectively, were approximately two times higher than those of the contribution percent, and this significant distinction was mainly caused by the variation of nitrate: the contribution of Tagr NH_3 to nitrate was generally below 10%, as shown in Table 2, but the reduction of nitrate associated with removing Tagr NH_3 emissions could exceed 95%, as shown in Table 3. This difference between the results of ISAM and brute-force was expected as a result of high nonlinearity in the NO_x chemistry. The nitrate formation could become more sensitive when the "rich NH_3" environment shifts to a "poor NH_3" environment, which means the decrease of the nitrate mass burden would accelerate with the NH_3 emissions reduction. Therefore, it can be deduced that the contribution of NH_3 to nitrate should be significantly lower under a "rich NH_3" environment than that under a "poor NH_3" environment. A similar phenomenon was also reported in previous studies (Wang et al., 2011; Xu et al., 2016). To prove this point, further brute-force sensitivity tests were conducted. The variations of sulfate, nitrate, ammonium, and SNA mass burden associated with the reduction of NH_3 emissions (80%, 50%, 40%, 30%, 20%, and 10% TA NH_3 emission,

https://doi.org/10.5194/acp-2019-1128
Preprint. Discussion started: 16 March 2020

Atmospheric Chemistry and Physics Discussions

respectively) is shown in Figure 8. It can be seen that the decrease in nitrate mass concentration was more rapid than that of ammonium, and the trend became slightly faster with the reduction of NH_3 emissions (signifying the transition from a "rich NH_3" to a "poor NH_3" environment) in the regions with a high mass burden of NH_3: BTH, NEC, SCB, and SDP. Furthermore, this acceleration stopped while 20% of NH_3 emissions remained.

5. Conclusions

The emission budget of agriculture NH_3 was huge and played an important role on the regional particle pollution in China. As a precursor of the secondary aerosol, reasonably estimate the nonlinear processes of secondary aerosol formation should be the key point for capturing the contribution of NH_3 to particle pollution. In this study, the air quality modeling system RAMS-CMAQ was applied to simulate spatial-temporal distribution of trace gas and aerosols in 2015. In addition, the PKU-NH_3 emission inventory which compiled on 1km×1km horizontal resolution with monthly based data was applied to accurately capture the agriculture NH_3 emission features in China. Then, the source apportionment module ISAM was coupled into this modeling system to quantitatively estimate the contribution of agriculture NH_3 to $PM_{2.5}$ mass burden. The brute-force sensitivity tests were also conducted for discussing the impact of the agriculture NH_3 emission reduction. The meteorological factors and mass concentration of NH_3, SO_2, NO_2, and $PM_{2.5}$ from simulation were evaluated and showed well agreement with the observation data. Some interesting results were explored and summarized as follow:

(1) The high mass burden of NH_3 could exceeded 10 μg m^{-3}, and mainly appeared in the NCP, CNC, YRD, and SCB. These regions were highly coincidence with the regions that heavy particle pollution covered in China. Therefore, it can be deduced that the influence of agriculture NH_3 on the $PM_{2.5}$ mass concentration should be significant.

(2) The results from ISAM simulation shows that the Tagr NH_3 provided 14-18% contribution to the $PM_{2.5}$ in the most part of east China, and the largest annual average contribution appeared in CNC (17.5%). Specific to the SNA components, the annually and regional average contribution of Tagr NH_3 to ammonium, nitrate, sulfate was 87.6%, 10.1%, and 2.2% in China. The agriculture NH_3 emission provided major contribution to the ammonium formation, but tiny contribution to the sulfate due to the various other ways of sulfate formation.

(3) The brute-force sensitive test could reflect the effect of changing Tagr NH_3 emission on $PM_{2.5}$ mass

https://doi.org/10.5194/acp-2019-1128
Preprint. Discussion started: 16 March 2020

Atmospheric Chemistry and Physics Discussions

burden. The results indicated that the reduction percent of $PM_{2.5}$ mass burden due to removal Tagr NH_3 emission could reach 23-35% in the most part of east China, which was approximately two times higher than the contribution. The reduction percent of nitrate that reached exceed 95% was the main reason caused this significant different. In addition, the further analysis proved that the ambient NH_3 mass burden could obviously affects its contribution to the SNA formation: the NH_3 contribution to nitrate should be lower under "rich NH_3" and higher under "poor NH_3". Therefore, the influence of NH_3 would enhance with the decreasing of ambient NH_3 mass concentration.

It is suggested that the influence of NH_3 on the $PM_{2.5}$ mass burden is complex because of the nonlinearity of secondary aerosol formation. Significant deviation exists between the results from ISAM and the brute-force method; therefore, these two kinds of results should be distinguished and applied to explain different issues: the contribution under the current scenario and the effect due to emissions reduction, respectively. The modeling system is a versatile tool that allows us to investigate this valuable information to choose more efficient strategies for reducing the impact of agricultural NH_3 and improving air quality.

Acknowledgments

This work was supported by the Strategic Priority Research Program of the Chinese Academy of Sciences (XDA19040204), and the National Natural Science Foundation of China (41830109).

https://doi.org/10.5194/acp-2019-1128
Preprint. Discussion started: 16 March 2020

Atmospheric Chemistry and Physics Discussions

330 **Appendix A**

331 The daily average temperature, relative humidity, wind speed and maximum wind direction in January
332 and July 2015 were compared with the surface shared data from the Chinese National Meteorological
333 Center (http://data.cma.cn/) in 9 stations. The comparison results are shown in Figure A1-A4. These stations
334 are located in the East China where the high NH_3 emission regions. Generally, the modeled temperature
335 was in good agreement with the observed data, and can reflect the large fluctuation and seasonal variation
336 of relative humidity as well, except that some of the extreme high or low values appeared abruptly. As
337 shown in Figure A3, most of the daily average wind speed was lower than 3 m s^{-1} at Zhengzhou, Jinan,
338 Miyun, and Baoding station (all located in the North China Plain), which means the diffusion condition was
339 not good due to the stable weather. Otherwise, the relatively strong wind appeared at Nanjing, Chaoyang,
340 Nanning, and Tianjin. The modeled wind speed generally reproduced all these features. The direct
341 comparison between observed and modeled wind direction which can be easily influenced by the
342 surrounding surface features is difficult. Nevertheless, the prevailing wind direction in different seasons
343 can be captured by the simulation results for all stations.
344
345
346
347
348
349
350
351
352
353
354
355
356
357
358
359

https://doi.org/10.5194/acp-2019-1128
Preprint. Discussion started: 16 March 2020

Atmospheric Chemistry and Physics Discussions

Reference

Babar, Z. B.; Park, J.; Lim, H. Influence of NH_3 on secondary organic aerosols from the ozonolysis and photooxidation of a -pinene in a flow reactor. *Atmos. Environ.* 2017, 164, 71-84, DOI: 10.1016/j.atmosenv.2017.05.034

Ball, S. M.; Hanson, D. R.; Eisele, F. L.; McMurry, P. H. Laboratory studies of particle nucleation: Initial results for H_2SO_4, H_2O, and NH_3 vapors. *J. Geophys. Res.* 1999, 104, 23709-23718, DOI: 10.1029/1999JD900411

Benson, D. R.; Yu, J. H.; Markovich, A.; Lee, S. H. Ternary homogeneous nucleation of H_2SO_4, NH_3, and H_2O under conditions relevant to the lower troposphere. *Atmos. Chem. Phys.* 2011, 11, 4755-4766, DOI: 10.5194/acp-11-4755-2011

Brost, R. A.; Delany, A. C.; Huebert, B. J. Numerical modeling of concentrations and fluxes of HNO_3, NH_3, and NH_4NO_3 near the ground. *J. Geophys. Res.* 1988, 93, 7137-7152, DOI: 10.1029/JD093iD06p07137

Cao, Z.; Zhou, X.; Ma, Y.; Wang, L.; Wu, R.; Chen, B.; Wang, W. The concentrations, formations, relationships and modeling of sulfate, nitrate and ammonium (SNA) aerosols over China. *Aerosol Air Qual. Res.* 2017, 17, 84-97, DOI: 10.4209/aaqr.2016.01.0020

Chen, Y.; Schleicher, N.; Cen, K.; Liu, X.; Yu, Y.; Zibat, V.; Dietze, V.; Fricker, M.; Kaminski, U.; Chen, Y.; Chai, F.; Norra, S. Evaluation of impact factors on $PM_{2.5}$ based on long-term chemical components analyses in the megacity Beijing, China. *Chemosphere* 2016, 155, 234-242, DOI: 10.1016/j.chemosphere.2016.04.052

Chang, J. The role of H_2O and NH_3 on the formation of NH_4NO_3 aerosol particles and De-NOx under the corona discharge treatment of combustion flue gases. *J. Aerosol Sci.* 1989, 20, 1087-1090, DOI: 10.1016/0021-8502(89)90768-4

Cotton, W.; Pielke, R.; Walko, G.; Liston, G.; Tremback, C.; Jiang, H.; McAnelly, R.; Harrington, J.; Nicholls, M.; Carrio, G.; McFadden, J. RAMS 2001: current status and future directions, Meteorol. *Atmos. Phys.* 2003, 82, 5-29, DOI:

DeFoy, B.; Lu, Z.; and Streets, D. G. Satellite NO_2 retrievals suggest China has exceeded its NO_x reduction goals from the twelfth five-year plan. *Sci. Rep.* 2016, 6, 35912, DOI: 10.1007/s00703-001-0584-9

Eder, B.; Yu S. A performance evaluation of the 2004 release of Models-3 CMAQ. *Atmos. Environ.* 2006, 40, 4811-4824, DOI: 10.1016/j.atmosenv.2005.08.045

Fountoukis, C.; Nenes, A. ISORROPIA II: a computationally efficient thermodynamic equilibrium model for K^+-Ca^{2+}-Mg^{2+}-NH_4^+-Na^+-SO_4^{2-}-NO_3^- -Cl^--H_2O aerosols. *Atmos. Chem. Phys.* 2007, 7, 4639-4659, DOI: 10.5194/acp-7-4639-2007

Fu, X.; Wang, S.; Xing, J.; Zhang, X.; Wang, T.; Hao, J. Increasing Ammonia Concentrations Reduce the Effectiveness of Particle Pollution Control Achieved via SO_2 and NO_x Emissions Reduction in East China. *Environ. Sci. Technol.* 2017, 4, 221-227, DOI: 10.1021/acs.estlett.7b00143

Huang, X.; Song, Y.; Li, J.; Huo, Q.; Cai, X.; Zhu, T.; Hu, M.; Zhang, H. A high-resolution ammonia emission inventory in China. *Global Biogeochem. Cy.* 2012, 26, 1030-1044, DOI: 10.1029/2011GB004161

Kang, Y.; Liu, M.; Song, Y.; Huang, X.; Yao, H.; Cai, X.; Zhang, H.; Kang, L.; Liu, X.; Yan, X.; He, H.; Zhang, Q.; Shao, M.; Zhu, T. High-resolution ammonia emissions inventories in China from 1980 to 2012. *Atmos. Chem. Phys.* 2016, 16, 2043-2058, DOI: 10.5194/acpd-15-26959-2015

Koo, B.; Wilson, G.; Morris, R.; Dunker, A.; Yarwood, G. Comparison of Source Apportionment and Sensitivity Analysis in a Particulate Matter Air Quality Model. *Environ. Sci. Technol.* 2009, 43, 6669-6675

Kurokawa, J.; Ohara, T.; Morikawa, T.; Hanayama, S.; Maenhout, G.; Fukui, T.; Kawashima, K.; Akimoto, H. Emissions of air pollutants and greenhouse gases over Asian regions during 2000-2008: Regional Emission inventory in ASia (REAS) version 2. *Atmos. Chem. Phys.* 2013, 13, 11019-11058, DOI: 10.5194/acp-13-11019-2013

Kulmala, M.; Korhonen, P.; Napari, I.; Karlsson, A.; Berresheim, H.; O'Dowd, C. D. Aerosol formation during PARFORCE: Ternary nucleation of H_2SO_4, NH_3, and H_2O. *J. Geophys. Res.* 2002, 107, DOI: 10.1029/2001JD000900.

Lai, S.; Zhao, Y.; Ding, A.; Zhang, Y.; Song, T.; Zheng, J.; Ho, K. F.; Lee, S.; Zhong, L. Characterization of $PM_{2.5}$ and the major chemical components during a 1-year campaign in rural Guangzhou. *Southern China, Atmos. Res.* 2016, 167,

https://doi.org/10.5194/acp-2019-1128
Preprint. Discussion started: 16 March 2020

Atmospheric Chemistry and Physics Discussions

208-215, DOI: 10.1016/j.atmosres.2015.08.007

Lei, Y.; Zhang, Q.; He, K.; Streets, D. Primary anthropogenic aerosol emission trends for China, 1990-2005. *Atmos. Chem. Phys.* 2011, 11, 931-954, DOI: 10.5194/acp-11-931-2011

Liu, M.; Huang, X.; Song, Y.; Tang, J.; Cao, J.; Zhang, X.; Zhang, Q.; Wang, S.; Xu, T.; Kang, L.; Cai, X.; Zhang, H.; Yang, F.; Wang, H.; Yu, J.; Lau, A.; He, L.; Huang, X.; Duan, L.; Ding, A.; Xue, L.; Gao, J.; Liu, B.; Zhu, T. Ammonia emission control in China would mitigate haze pollution and nitrogen deposition, but worsen acid rain. *PNAS*, 2019, 116, 7760-7765, DOI: 10.1073/pnas.1814880116

Lu, Z.; Zhang, Q.; Streets, D. G. Sulfur dioxide and primary carbonaceous aerosol emissions in China and India, 1996-2010. *Atmos. Chem. Phys.* 2011, 11, 9839-9864, DOI:

Mathur, R.; Yu, S.; Kang, D.; Schere, K. Assessment of the winter-time performance of developmental particulate matter forecasts with the Eta-CMAQ modeling system. *J. Geophys. Res.* 2008, 113, DOI: 10.1029/2007JD008580,

McMurry, P. H.; Takano, H.; Anderson, G. R. Study of the ammonia (gas)-sulfuric acid (aerosol) reaction rate. *Environ. Sci. Technol.* 1983, 17, 347-352, DOI: 10.1021/es00112a008

Paulot, F.; Jacob, D. J.; Pinder, R. W.; Bash, J. O.; Travis, K.; Henze, D. K. Ammonia emissions in the United States, European Union, and China derived by high-resolution inversion of ammonium wet deposition data: Interpretation with a new agricultural emissions inventory (MASAGE_NH3). *J. Geophys. Res.* 2014, 119, 4343-4364, DOI: 10.1002/2013JD021130

Pen, Y.; Tian, S.; Zhao, Y.; Zhang, L.; Zhu, X.; Gao, J.; Huang, W.; Zhou, Y.; Song, Y.; Zhang, Q.; Wang, Y. Identifying ammonia hotspots in China using a national observation network. Environ. Sci. Technol. 2008, doi: 10.1021/acs.est.7b05235, DOI: 10.1021/acs.est.7b05235

Quan, J.; Tie, X.; Zhang, Q.; Liu, Q.; Li, X.; Gao, Y.; Zhao, D. Characteristics of heavy aerosol pollution during the 2012–2013 winter in Beijing, China. *Atmos. Environ.* 2014, 88, 83-89, DOI: 10.1016/j.atmosenv.2014.01.058

Ren, H.; Zhang, L.; Hong, X. Politic recommendations on strengthening reduction of air pollutant emissions in China. *Environ. Sustain. Dev.* 2014, 39, 4-13, (in Chinese)

Tao, M.; Chen, L.; Xiong, X.; Zhang, M.; Ma, P.; Tao, J.; Wang, Z. Formation process of the widespread extreme haze pollution over northern China in January 2013: Implications for regional air quality and climate. *Atmos. Environ.* 2014, 98, 417-425, DOI: 10.1016/j.atmosenv.2014.09.026

Tanner, R. L.; Leaderer, B. P.; Spengler, J. D. Acidity of atmospheric aerosols. *Environ. Sci. Technol.* 1981, 15, 1150–1153, DOI: 10.1021/es00092a003

van der Werf, G.; Randerson, J. Giglio, L.; Collatz, G.; Mu, M.; Kasibhatla, P.; Morton, D.; Defries, R.; Jin, Y.; van Leeuwen, T. Global fire emissions and the contribution of deforestation, savanna, forest, agricultural, and peat fires (1997-2009). *Atmos. Chem. Physics.* 2010, 10, 11707-11735, DOI: 10.5194/acp-10-11707-2010

Wang, G.; Zhang, R.; Gomez, M. E.; Yang, L.; Levy Zamora, M.; Hu, M.; Lin, Y.; Peng, J.; Guo, S.; Meng, J.; Li, J.; Cheng, C.; Hu, T.; Ren, Y.; Wang, Y.; Gao, J.; Cao, J.; An, Z.; Zhou, W.; Li, G.; Wang, J.; Tian, P.; Marrero-Ortiz, W.; Secrest, J.; Du, Z.; Zheng, J.; Shang, D.; Zeng, L.; Shao, M.; Wang, W.; Huang, Y.; Wang, Y.; Zhu, Y.; Li, Y.; Hu, J.; Pan, B.; Cai, L.; Cheng, Y.; Ji, Y.; Zhang, F.; Rosenfeld, D.; Liss, P. S.; Duce, R. A.; Kolb, C. E.; Molina, M. J. Persistent sulfate formation from London Fog to Chinese haze. *Proc. Natl. Acad. Sci.* 2016, 113, 13630-13635, DOI: 10.1073/pnas.1616540113

Wang, H.; Qiao, L.; Lou, S.; Zhou, M.; Ding, A.; Huang, H.; Chen, J.; Wang, Q.; Tao, S.; Chen, C.; Li, L.; Huang, C.; 2016, Chemical composition of $PM_{2.5}$ and meteorological impact among three years in urban Shanghai, China. *J. Clean. Prod.* 2016, 112, 1302-1311, DOI: 10.1016/j.jclepro.2015.04.099

Wang, S.; Zhang, Q.; Martin, R.V.; Philip, S.; Liu, F.; Li, M.; Jiang, X.; He, K. Satellite measurements oversee China's sulfur dioxide emission reductions from coal-fired power plants. *Environ. Res. Lett.* 2015, 10, doi: 10.1088/1748-9326/10/11/114015, DOI:

https://doi.org/10.5194/acp-2019-1128
Preprint. Discussion started: 16 March 2020

Atmospheric Chemistry and Physics Discussions

448 Wang, S.; Xing, J.; Jang, C.; Zhu, Y.; Fu, J.; Hao, J. Impact Assessment of Ammonia Emissions on Inorganic Aerosols in
449 East China Using Response Surface Modeling Technique. *Environ. Sci. Technol.* 2011, 45, 9293-9300, DOI:
450 10.1021/es2022347
451 Wang, Z.; Chien, C.; Tonnesen, G. Development of a tagged species source apportionment algorithm to characterize three-
452 dimensional transport and transformation of precursors and secondary pollutants. *J. Geophys. Res.* 2009, 114, DOI:
453 10.1029/2008JD010846,
454 Whitten, G.; Heo, G.; Kimura, Y.; McDonald-Buller, E.; Allen, D.; Carter, W. P. L.; Yarwwod, G. A new condensed toluene
455 mechanism for Carbon Bond: CB05-TU. *Atmos. Environ.* 2010, 44, 5346-5355, DOI:
456 10.1016/j.atmosenv.2009.12.029
457 Wu, S.; Hu, J.; Zhang, Y.; Aneja, V. P. Modeling atmospheric transport and fate of ammonia in North Carolina-Part II:
458 Effect of ammonia emissions on fine particulate matter formation. *Atmos. Environ.* 2008, 42, 3437-3451, DOI:
459 10.1016/j.atmosenv.2007.04.022
460 Xia, Y.; Zhao, Y.; and Nielsen, C. P. Benefits of China's efforts in gaseous pollutant control indicated by the bottom-up
461 emissions and satellite observations 2000-2014. *Atmos. Environ.* 2016, 136, 43-53, DOI:
462 10.1016/j.atmosenv.2016.04.013
463 Xu, P.; Liao, Y. J.; Lin, Y. H.; Zhao, C. X.; Yan, C. H.; Cao, M. N.; Wang, G. S.; Luan, S. J. High-resolution inventory of
464 ammonia emissions from agricultural fertilizer in China from 1978 to 2008. Atmos. Chem. Phys. 2016, 16, 1207-
465 1218, DOI: 10.5194/acpd-15-25299-2015
466 Yang, Y.; Wilkinson, J.; Russell. A. Fast, Direct Sensitivity Analysis of Multi-Dimensional Photochemical Models.
467 *Environ. Sci. Technol.* 1997, 31, 2859-2868, DOI: 10.1021/es970117w
468 Zhao, Z.; Bai, Z.; Winiwarter, W.; Kiesewetter, G.; Heyes, C.; Ma, L. Mitigating ammonia emission from agriculture
469 reduces $PM_{2.5}$ pollution in the Hai River Basin in China. *Sci. Total Environ.* 2017, 609, 1152-1160, DOI:
470 10.1016/j.scitotenv.2017.07.240
471 Zhao, X. J.; Zhao, P. S.; Xu, J.; Meng, W.; Pu, W. W.; Dong, F.; He, D.; Shi, Q. F. Analysis of a winter regional haze event
472 and Its formation mechanism in the North China Plain. *Atmos. Chem. Phys.* 2013, 13, 5685–5696, DOI: 10.5194/acp-
473 13-5685-2013
474 Zhang, J. K.; Sun, Y.; Liu, Z. R.; Ji, D. S.; Hu, B.; Liu, Q.; Wang, Y. S. Characterization of submicron aerosols during a
475 month of serious pollution in Beijing, 2013. *Atmos. Chem. Phys.* 2014, 14, 2887–2903, DOI: 10.5194/acp-14-2887-
476 2014.
477 Zhang, K.; Ma, Y.; Xin, J.; Liu, Z.; Ma, Y.; Gao, D.; Wu, J.; Zhang, W.; Wang, Y.; Shen, P. The aerosol optical properties
478 and $PM_{2.5}$ components over the world's largest industrial zone in Tangshan, North China. *Atmos. Res.* 2018, 201, 226-
479 234, DOI: 10.1016/j.atmosres.2017.10.025
480 Zhang, L.; Chen, Y.; Zhao, Y.; Henze, D.; Zhu, L.; Song, Y.; Paulot, F.; Liu, X.; Pan, Y.; Lin, Y.; Huang, B. Agricultural
481 ammonia emissions in China: reconciling bottom-up and top-down estimates. *Atmos. Chem. Phys.* 2018, 18, 339-355,
482 DOI: 10.5194/acp-18-339-2018
483 Pan, Y.; Tian, S.; Zhao, Y.; Zhang, L.; Zhu, X.; Gao, J.; Huang, W.; Zhou, Y.; Song, Y.; Zhang, Q.; Wang, Y. Identifying
484 ammonia hotspots in China using a national observation network. *Environ. Sci. Technol.* 2018, doi:
485 10.1021/acs.est.7b05235, DOI: 10.1021/acs.est.7b05235
486 Zhang, X.; Wang, Y.; Niu, Y.; Zhang, X.; Gong, S.; Zhang, Y.; Sun, J. Atmospheric aerosol compositions in China:
487 spatial/temporal variability, chemical signature, regional haze distribution and comparisons with global aerosols.
488 *Atmos. Chem. Phys.* 2012, 12, 779-799, DOI: 10.5194/acp-12-779-2012
489 Zhou, F.; Ciais, P.; Hayashi, K.; Galloway, J.; Kim, D.; Yang, L.; Li, S.; Liu, B.; Shang, Z.; Gao, S. Re-estimating NH_3
490 emissions from Chinese cropland by a new nonlinear model. *Environ. Sci. Technol.* 2016, 50, 564-572, DOI:
491 10.1021/acs.est.5b03156

https://doi.org/10.5194/acp-2019-1128
Preprint. Discussion started: 16 March 2020

Atmospheric Chemistry and Physics Discussions

492 Zhou, Y.; Cheng, S.; Lang, J.; Chen, D.; Zhao, B.; Liu, C.; Xu, R.; Li, T. A comprehensive ammonia emission inventory
493 with high-resolution and its evaluation in the Beijing–Tianjin–Hebei (BTH) region, China. *Atmos. Environ.* 2015,
494 106, 305-317, DOI: 10.1016/j.atmosenv.2015.01.069
495 Xu, P.; Koloutsou-Vakakis, S.; Rood, M.; Luan, S. Projections of NH_3 emissions from manure generated by livestock
496 production in China to 2030 under six mitigation scenarios. *Sci. Total Environ.* 2017, 31, 78-86, DOI:
497 10.1016/j.scitotenv.2017.06.258
498 Zheng, B.; Tong, D.; Li, M.; Liu, F.; Hong, C.; Geng, G.; Li, H.; Li, X.; Peng, L.; Qi, J.; Yan, L.; Zhang, Y.; Zhao, H.;
499 Zheng, Y.; He, K.; Zhang, Q. Trends in China's anthropogenic emissions since 2010 as the consequence of clean air
500 actions. *Atmos. Chem. Phys.* 2018, 18, 14095-14111, DOI: 10.5194/acp-18-14095-2018
501 Kurokawa, J.; Ohara, T.; Morikawa, T.; Hanayama, S.; Janssens-Maenhout, G.; Fukui, T.; Kawashima, K.; Akimoto, H.
502 Emissions of air pollutants and greenhouse gases over Asian regions during 2000-2008: Regional Emission inventory
503 in ASia (REAS) version 2. *Atmos. Chem. Phys.* 2013, 13, 11019-11058, DOI: 10.5194/acp-13-11019-2013
504 Fu, X.; Wang, S.; Ran, L.; Pleim, J.; Cooter, E.; Bash, J.; Benson, V.; Hao, J. Estimating NH_3 emissions from agricultural
505 fertilizer application in China using the bi-directional CMAQ model coupled to an agro-ecosystem model. *Atmos.*
506 *Chem. Phys.* 2015, 15, 6637-6649, DOI: 10.5194/acp-15-6637-2015
507
508
509
510
511
512
513
514
515
516
517
518
519
520
521
522
523
524
525
526

https://doi.org/10.5194/acp-2019-1128
Preprint. Discussion started: 16 March 2020

Atmospheric Chemistry and Physics Discussions

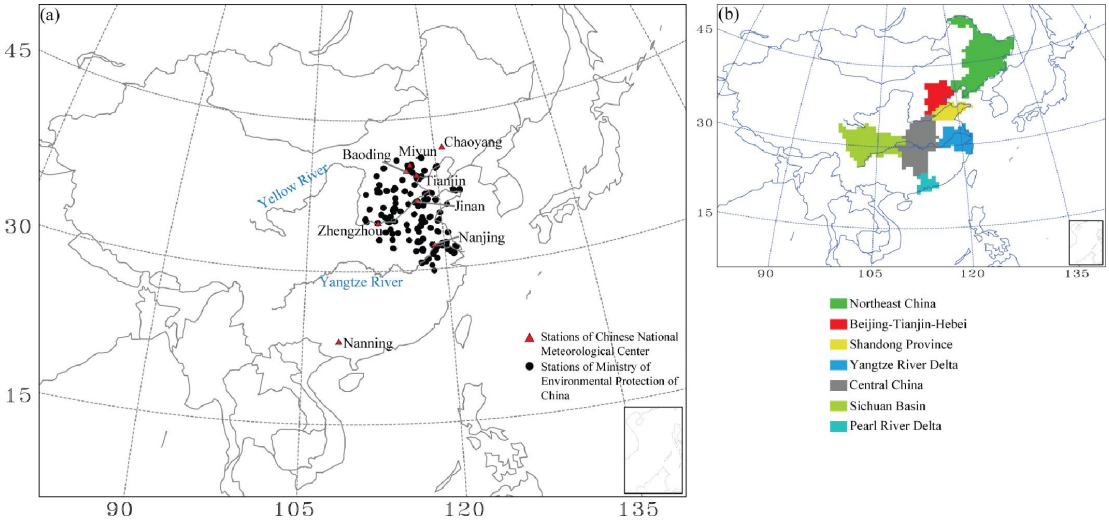

Figure 1. Model domain used in this study and the geographic locations of Northeast China, Beijing-Tianjin-Hebei, Shandong Province, Yangtze River Delta, Central China, Sichuan Basin, and Pearl River Delta. The location of observation data was also shown in the model domain.

https://doi.org/10.5194/acp-2019-1128
Preprint. Discussion started: 16 March 2020

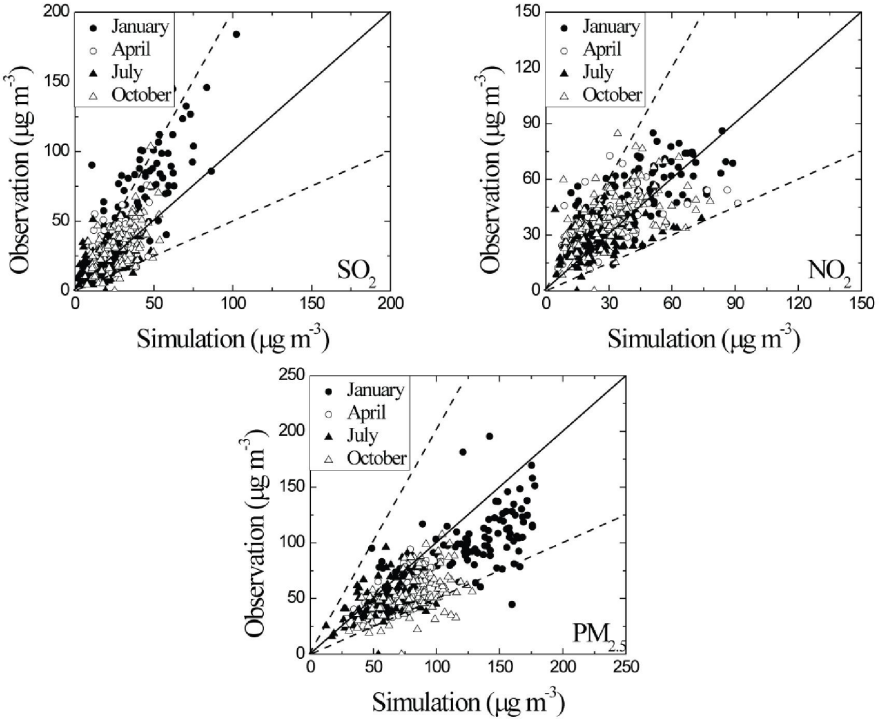

Figure 2. The scatter plots between the modeled and the observed monthly SO_2, NO_2, and $PM_{2.5}$ in 2015. The solid lines are 1:1 and the dashed lines are 2:1 or 1:2.

https://doi.org/10.5194/acp-2019-1128
Preprint. Discussion started: 16 March 2020

Atmospheric Chemistry and Physics Discussions

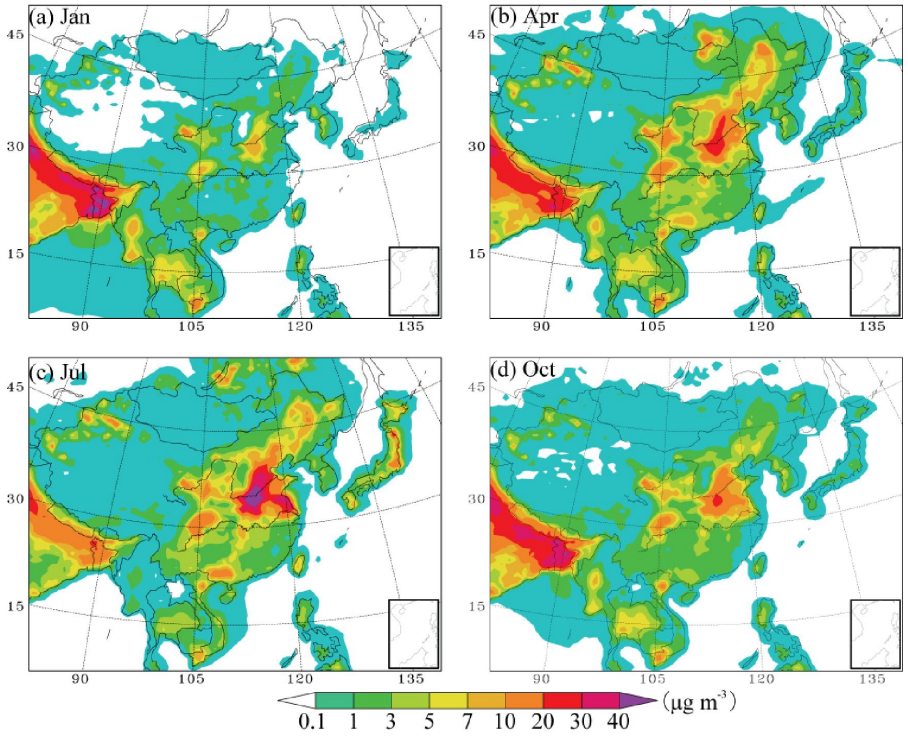

Figure 3. The horizontal distributions of the modeled monthly NH_3 mass concentration in January, April, July, and October in 2015.

https://doi.org/10.5194/acp-2019-1128
Preprint. Discussion started: 16 March 2020

Atmospheric Chemistry and Physics Discussions

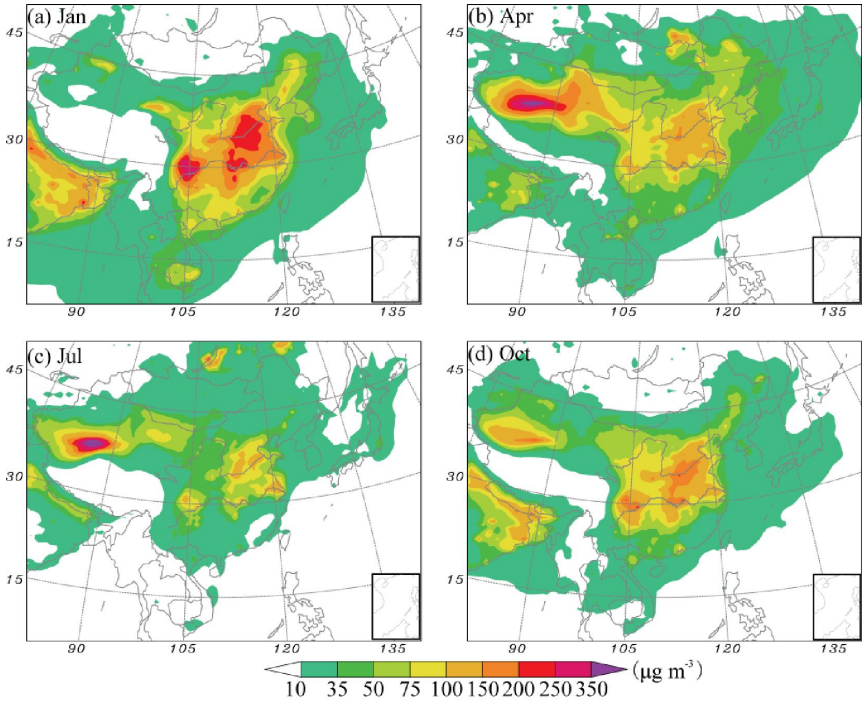

Figure 4. The horizontal distributions of the modeled monthly $PM_{2.5}$ mass concentration in January, April, July, and October in 2015.

https://doi.org/10.5194/acp-2019-1128
Preprint. Discussion started: 16 March 2020

Atmospheric Chemistry and Physics Discussions

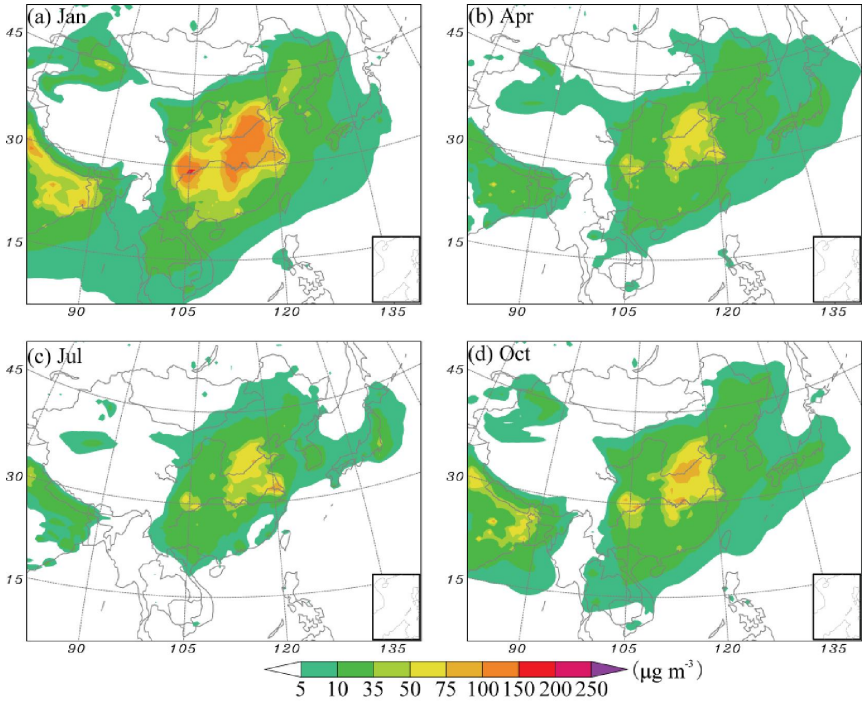

Figure 5. The horizontal distributions of the modeled monthly SNA mass concentration in January, April, July, and October in 2015.

https://doi.org/10.5194/acp-2019-1128
Preprint. Discussion started: 16 March 2020

Atmospheric Chemistry and Physics Discussions

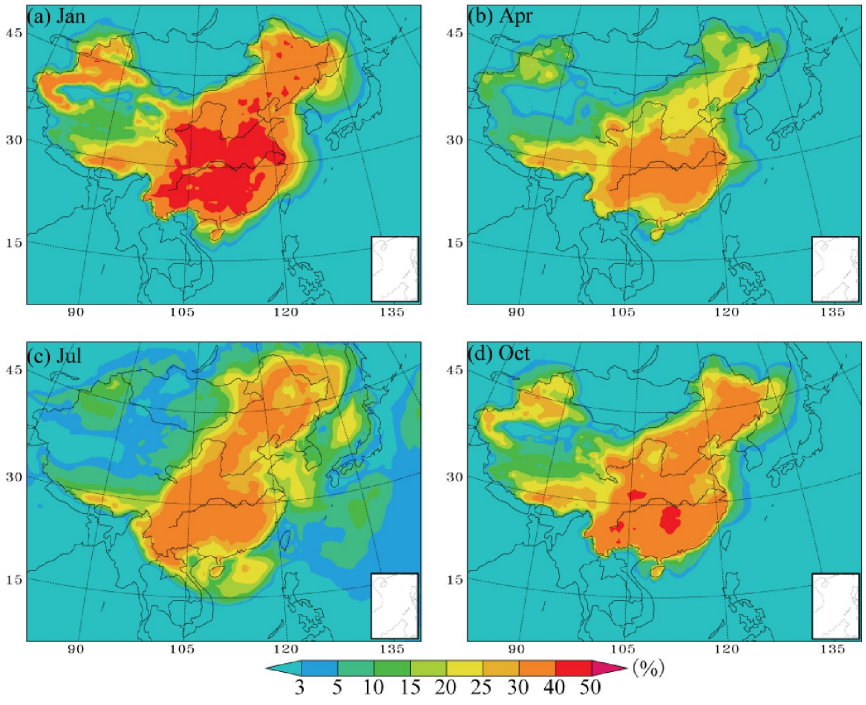

Figure 6. The horizontal distributions of the contribution percentage of NH_3 emissions to SNA mass concentration (%) in January and July.

https://doi.org/10.5194/acp-2019-1128
Preprint. Discussion started: 16 March 2020

Atmospheric Chemistry and Physics Discussions

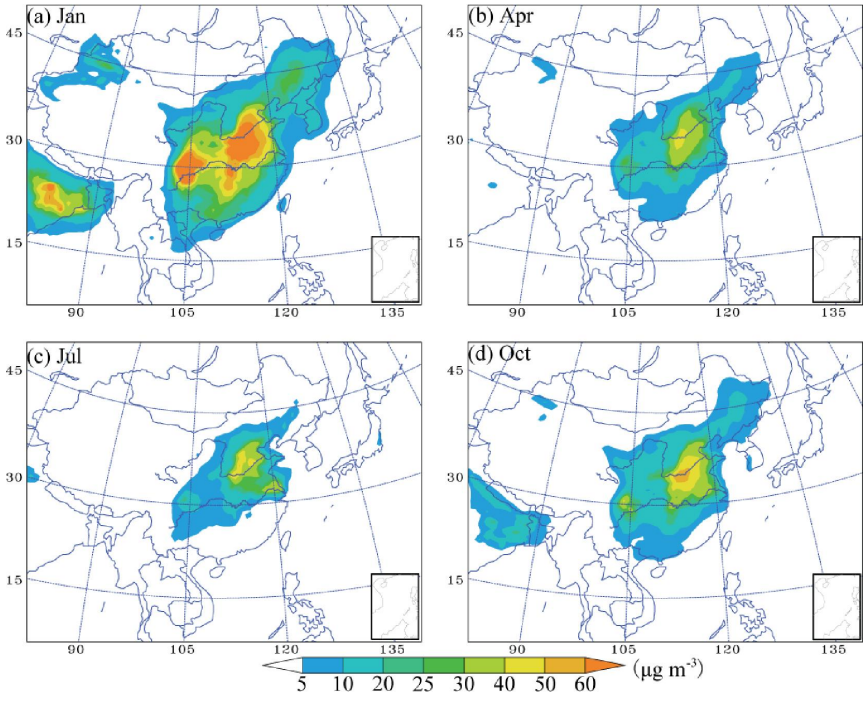

Figure 7. The horizontal distributions of SNA mass concentration (μg m^{-3}) variation associated with agriculture NH_3 removal in January and July.

https://doi.org/10.5194/acp-2019-1128
Preprint. Discussion started: 16 March 2020

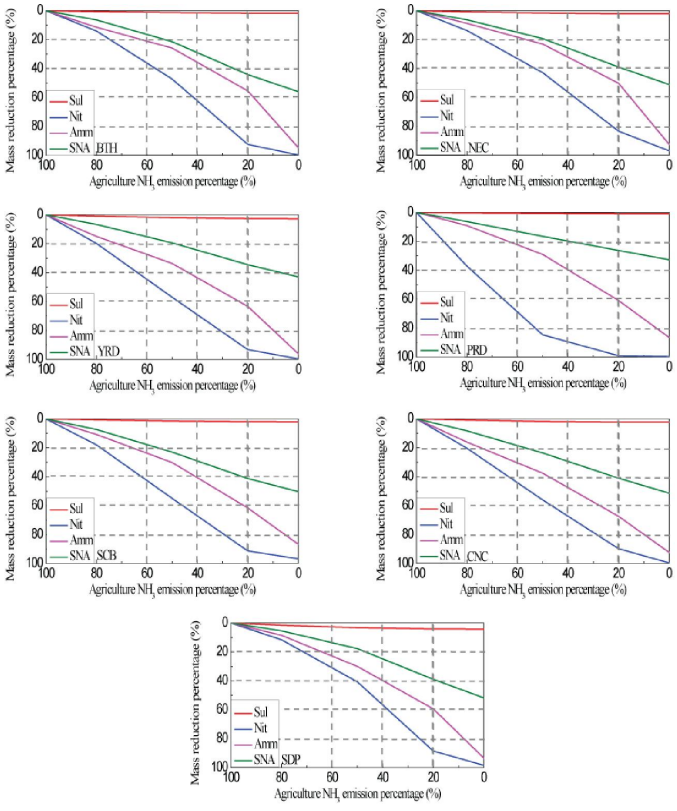

Figure 8. The variation (%) of sulfate, nitrate, ammonium, and SNA mass burden associated with the NH_3 emission reduction (%).

https://doi.org/10.5194/acp-2019-1128
Preprint. Discussion started: 16 March 2020

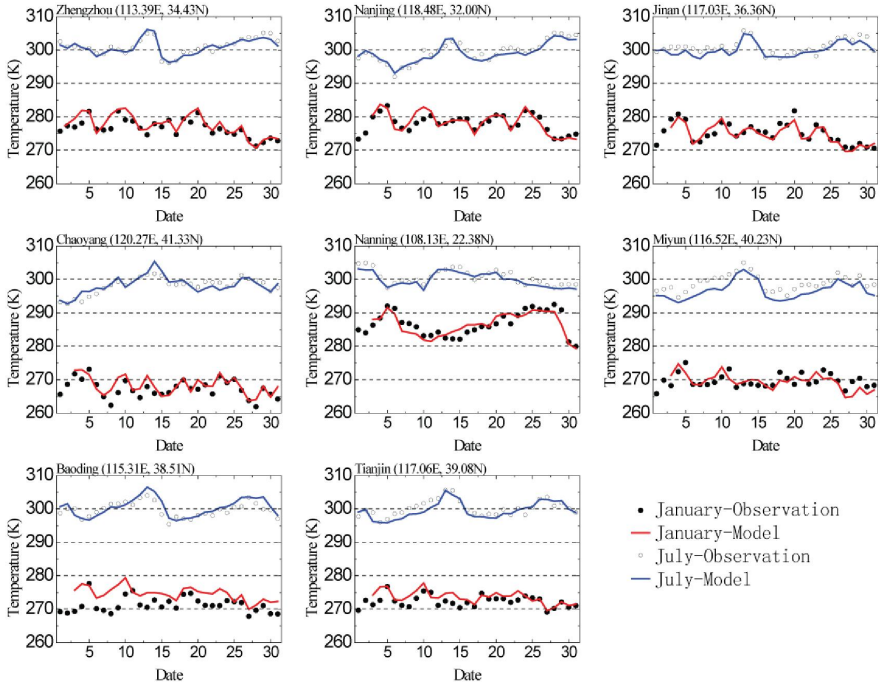

Figure A1. Observed and modeled daily average temperatures (K) in January and July 2015.

https://doi.org/10.5194/acp-2019-1128
Preprint. Discussion started: 16 March 2020

Atmospheric Chemistry and Physics Discussions

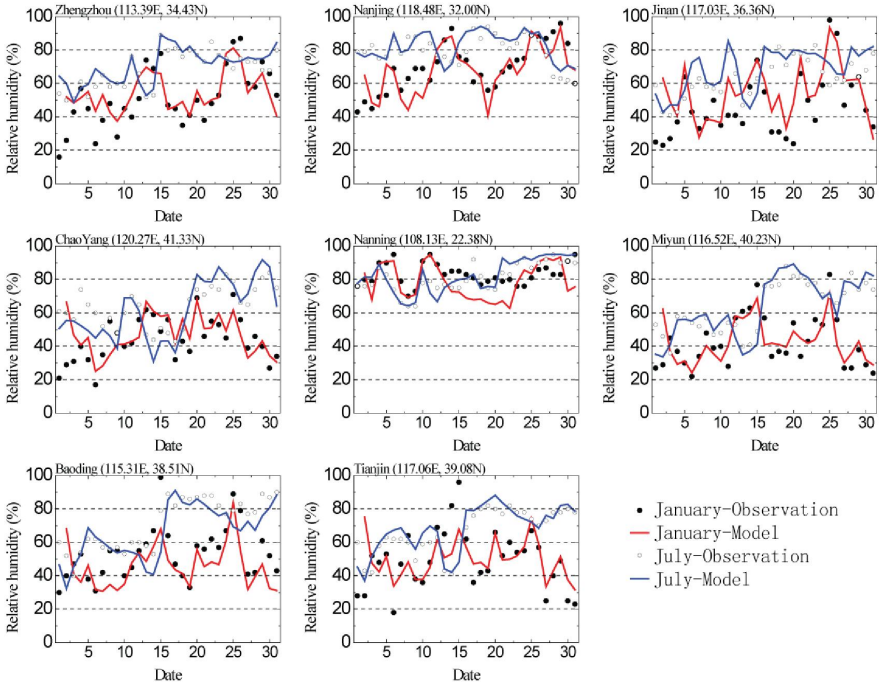

Figure A2. Same as Figure A1 but for relative humidity (%)

https://doi.org/10.5194/acp-2019-1128
Preprint. Discussion started: 16 March 2020

Atmospheric Chemistry and Physics Discussions

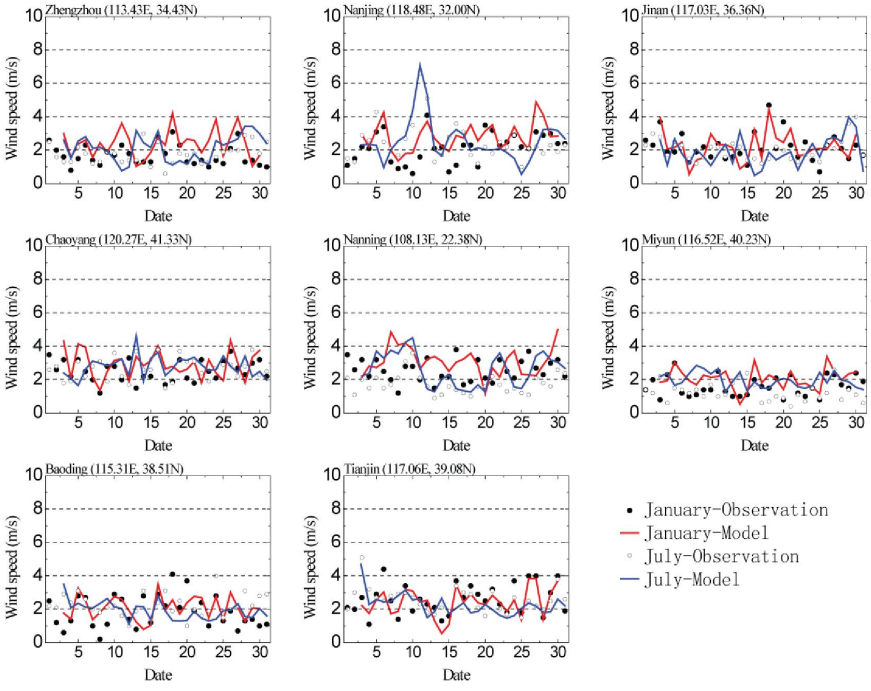

Figure A3. Same as Figure A1 but for wind speed (m s^{-1})

https://doi.org/10.5194/acp-2019-1128
Preprint. Discussion started: 16 March 2020

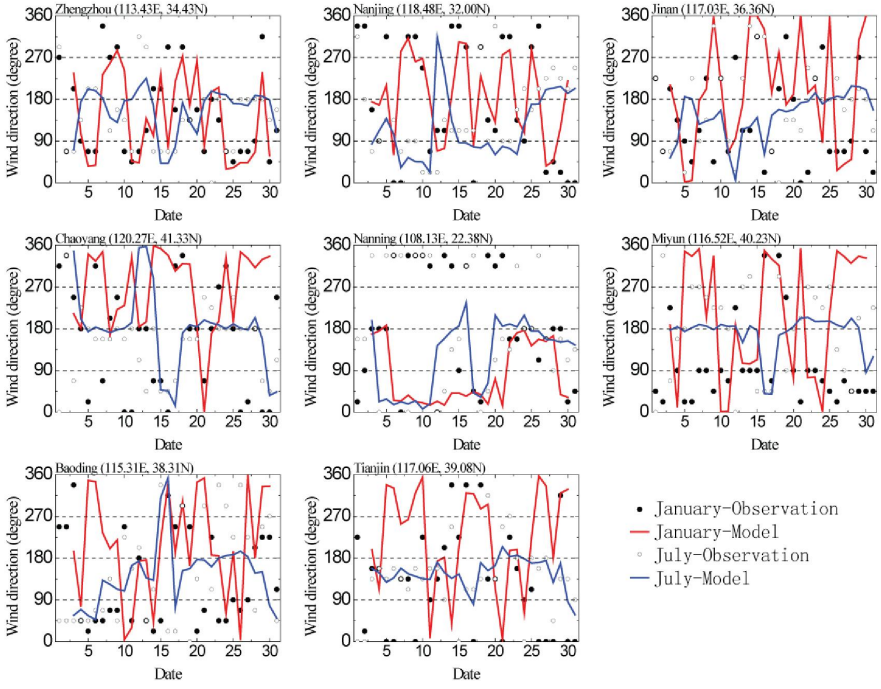

Figure A4. Same as Figure A1 but for daily maximum wind direction (degree)

https://doi.org/10.5194/acp-2019-1128
Preprint. Discussion started: 16 March 2020

Atmospheric Chemistry and Physics Discussions

802 Table 1. Statistical summary of the comparisons of the monthly average $PM_{2.5}$ between simulation and observation

		N^a	M^b	O^c	$\sigma_m{}^d$	$\sigma_o{}^e$	R^f	FB^g	NMB^h
$PM_{2.5}$	Jan	101	128.3	100.1	34.9	28.3	0.60	0.2	28.2
	Apr	101	74.9	58.4	15.4	15.2	0.67	0.3	28.3
	Jul	100	58.6	50.3	17.6	16.0	0.52	0.1	16.6
	Oct	100	81.0	54.8	23.1	19.7	0.52	0.4	47.9
NO_2	Jan	101	42.5	51.7	19.4	16.2	0.65	-0.2	-17.8
	Apr	101	27.8	35.0	15.7	11.5	0.57	-0.3	-20.5
	Jul	100	24.3	26.5	13.2	9.2	0.50	-0.2	-8.4
	Oct	100	33.2	42.0	16.4	14.9	0.53	-0.3	-20.9
SO_2	Jan	101	39.9	69.1	18.7	42.4	0.71	-0.5	-42.2
	Apr	101	22.9	31.2	10.1	12.7	0.51	-0.3	-26.6
	Jul	100	17.8	20.3	10.9	10.4	0.46	-0.2	-12.5
	Oct	100	27.0	31.5	12.3	16.7	0.63	-0.1	-14.4

803 [a] Number of samples
804 [b] Total mean of observation
805 [c] Total mean of simulation
806 [d] Standard deviation of observation
807 [e] Standard deviation of simulation
808 [f] Correlation coefficient between daily observation and simulation
809 [g] Fractional Bias
810 [h] Nmalized Mean Bias
811
812
813
814
815
816
817
818
819
820
821
822
823
824
825
826
827
828
829
830
831
832

https://doi.org/10.5194/acp-2019-1128
Preprint. Discussion started: 16 March 2020

Atmospheric Chemistry and Physics Discussions

833 Table 2. The regional percent (%) of T contribution to sulfate, nitrate, ammonium, and SNA mass concentration.

	Sulfate	Nitrate	Ammonium	SNA	$PM_{2.5}$
BTH	1.1	8.0	83.3	31.9	15.5
NEC	1.0	5.6	83.7	28.1	14.3
YRD	1.0	7.4	85.7	29.2	15.3
PRD	0.9	5.8	90.6	33.5	14.2
SCB	0.7	5.1	93.9	32.6	13.0
CNC	0.9	6.0	92.8	36.6	17.5
SDP	0.9	7.1	80.5	30.1	15.1
China	2.2	10.1	87.6	29.0	16.0

834
835
836
837
838
839
840
841
842
843
844
845
846
847
848
849
850
851
852
853
854
855
856
857
858
859
860
861
862
863
864
865
866
867

https://doi.org/10.5194/acp-2019-1128
Preprint. Discussion started: 16 March 2020

Atmospheric Chemistry and Physics Discussions

868 Table 3. The variation percent (%) of sulfate, nitrate, ammonium, and SNA mass concentration associated with
869 agriculture NH_3 removal.

	Sulfate	Nitrate	Ammonium	SNA	$PM_{2.5}$
BTH	0.7	99.8	94.7	49.4	34.4
NEC	0.7	96.9	92.5	48.9	31.1
YRD	5.0	99.2	96.1	48.8	31.6
PRD	2.0	99.2	97.2	40.3	23.4
SCB	2.6	96.7	85.9	49.8	25.9
CNC	1.9	99.2	92.3	50.9	32.3
SDP	2.7	99.5	93.4	46.6	34.0
China	1.6	98.8	93.8	45.7	25.2

870
871
872
873
874
875
876
877